

A new method to study the EMC Effect using the F_2^n structure function

H. Szumila-Vance¹, I. Cloet², C. Keppel¹, S. Escalante³, N. Kalantarians³

¹Thomas Jefferson National Accelerator Facility, Newport News, VA

²Argonne National Laboratory, Argonne, IL

³Virginia Union University, Richmond, VA

Abstract

The persistently mysterious deviations from unity of the ratio of nuclear target structure functions to those of deuterium as measured in deep inelastic scattering (termed the “EMC Effect”) have become the canonical observable for studies of nuclear medium modifications to free nucleon structure in the valence regime. The structure function of the free proton is well known from numerous experiments spanning decades. The free neutron structure function, however, has remained difficult to access. Only recently has it been extracted in a systematic study of the global data within a parton distribution function extraction framework and is available from the CTEQ-Jefferson Lab (CJ) Collaboration. Here we leverage the latter to introduce a new method to study the EMC Effect in nuclei by re-examining existing data and by now determining the magnitude of the medium modifications to the free neutron and proton structure functions independently. From the extraction of the free neutron from world data, it is possible to examine the nuclear effects in deuterium and their contribution to our interpretation of the EMC Effect. In this study, we observe that the ratio of the deuteron to the sum of the free neutron and proton structure functions has some x_B and Q^2 dependencies implying that the magnitude of the standard EMC Effect is in part due to the nuclear effects of the deuteron and also exhibits some x_B and Q^2 dependence.

1 Introduction

Deep inelastic scattering (DIS) has produced a wealth of information on the partonic structure of nuclei spanning several decades of experiments. The EMC Effect, or the observed modification to the bound nucleon partonic structure as compared to that of the free nucleon, is a direct observation from these experiments. The EMC Effect is observed in the regime where x_B is from 0.3–0.7, and the magnitude is measured as the slope of the ratio of the F_2^A / F_2^d structure function where A is for the target nucleus and d is deuterium. It was previously anticipated that this slope should be flat, but the surprising results indicated there is an A -dependent slope. The interpretation of this modification has been the subject of many experiments and great theoretical efforts for several decades.

From DIS, a great deal of information is known about the proton, the neutron structure is less understood. A recent effort by the CTEQ-Jefferson Lab Collaboration has reviewed the world DIS data and extracted the free neutron structure function for all kinematics. Knowledge of the neutron structure function is essential for the next generation of future DIS experiments.

Using the newly obtained free neutron structure function from CJ15, the EMC Effect can be examined in a different way. The original SLAC E139 experiment is the only experiment to have published the measured cross sections in addition to the measured F_2^A / F_2^d ratios. By re-analyzing

the data starting from the cross sections of the SLAC E139 experiment, the EMC Effect can be understood in terms of the free proton and free neutron independently of the nuclear effects of deuterium. Fig. 1 shows the kinematics of the E139 experiment.

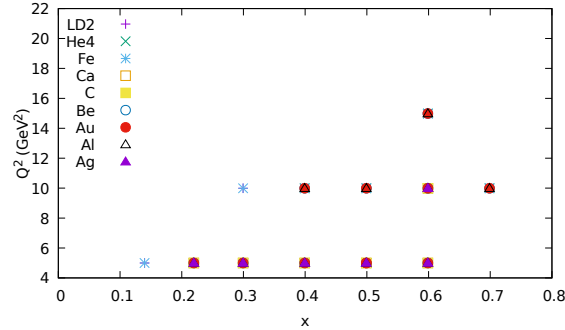


Figure 1: The kinematics x_B and Q^2 are shown from the SLAC E139 experiment for the target nuclei.

The kinematics span the range of x_B from approximately 0.1–0.7 and Q^2 from 2–15 GeV 2 depending on the target nucleus. The target nuclei include deuterium, helium, beryllium, carbon, calcium, iron, aluminum, silver, and gold.

2 Theory predictions using nuclear matter

Recent theoretical extractions of the F_2^d per nucleon are shown in Fig. 2. These results indicate that in the x_B range of interest to the EMC Effect (from 0.3–0.7), theoretical models show that nuclear modification of nearly 2% at $x_B < 0.6$, and the modification becomes quite large at values of x_B between 0.6–0.7. Additionally, the nuclear effects in deuterium alone do not follow a linear fit as has been applied to EMC data in this regime where F_2^d is the denominator.

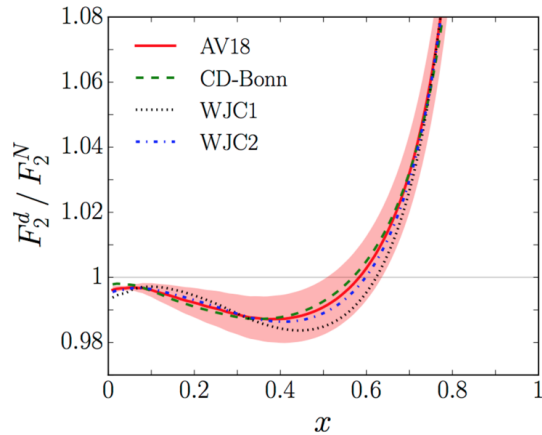


Figure 2: The theoretical extraction of the ratio of F_2^d / F_2^N . The deuteron exhibits some x_B -dependence such that the ratio is modified by approximately 2% in the regime of x_B between 0.3–0.7 (region of interest to the EMC Effect).

Beginning with quark models and choosing $Q^2 = 5 \text{ GeV}^2$, theoretically-derived F_2 ratios with respect to the free neutron and free proton are shown in Fig. 3.

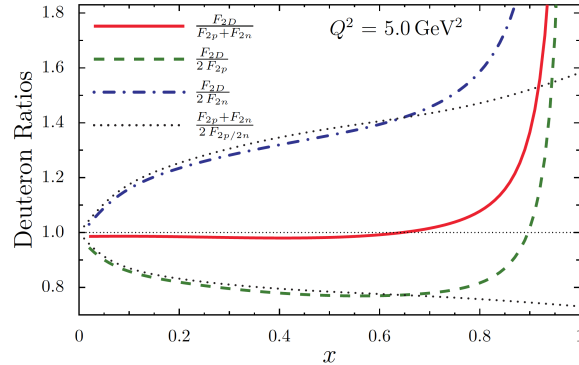


Figure 3: Theoretically-derived deuteron F_2 ratios with respect to the free neutron and proton, the free proton, and the free neutron are shown for $Q^2 = 5 \text{ GeV}^2$.

From the models shown in Fig. 3, the F_2 deuteron ratio with respect to the sum of the free neutron and free proton contributions is shown in red (and dips just below unity in the EMC Effect regime). By taking the ratio of $F_2^d/2F_2^p$ (shown in green), the slope dips far below unity and is greater in magnitude than the F_2 deuteron ratio shown in red. Taking $F_2^d/2F_2^n$ shows a positive slope that is of greater magnitude than $F_2^d/2F_2^p$.

3 F_2^n extraction and the CJ15 fit

Recent work by the CTEQ-Jefferson Lab (CJ) Collaboration reviewed the world DIS data on the proton and deuteron structure functions and extracted the free neutron structure function over the full range of kinematics. Through the application of the latest and best known deuteron nuclear corrections, the full global DIS data set provides the equivalent neutron data set. This extracted free neutron structure function enables the authors of this paper to examine the EMC Effect in a new way.

In Fig. 4, general comparisons of the newly extract F_2^n are made with respect to the F_2^p as derived by the NMC fit.

On the left of Fig. 4, the F_2^n and F_2^p for the same x_B and Q^2 kinematics is shown. The F_2^n in blue is the extracted points from the world data, and the F_2^p is the corresponding value (for the same kinematics) from the NMC fit. The overall x_B dependence is somewhat different as the neutron structure function is more comparable at larger x_B while the proton structure function drops off more sharply. The ratio of these quantities is shown on the right in Fig. 4 and agrees with previously extracted results.

3.1. Q^2 dependence

A significant observation in the CJ15-extracted structure functions is the Q^2 dependence. The proton structure function is shown on the left in Fig. 5 for various Q^2 from the CJ15 fit to the world DIS data. The corresponding deuteron structure function is shown on the right in Fig. 5. The SLAC E139 experiment took measurements at Q^2 in the range of 5–15 GeV^2 . The proton and

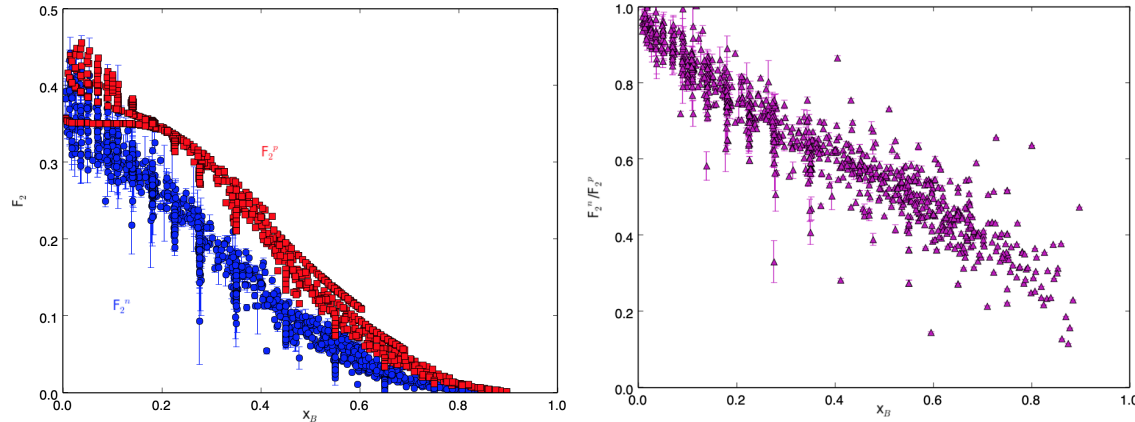


Figure 4: Left: The extracted F_2^n from the world DIS data is shown in blue, and the F_2^p from the NMC global fit is shown in red for the same corresponding x_B and Q^2 . Right: The ratio of the F_2^n / F_2^p from the left is shown as a function of x_B .

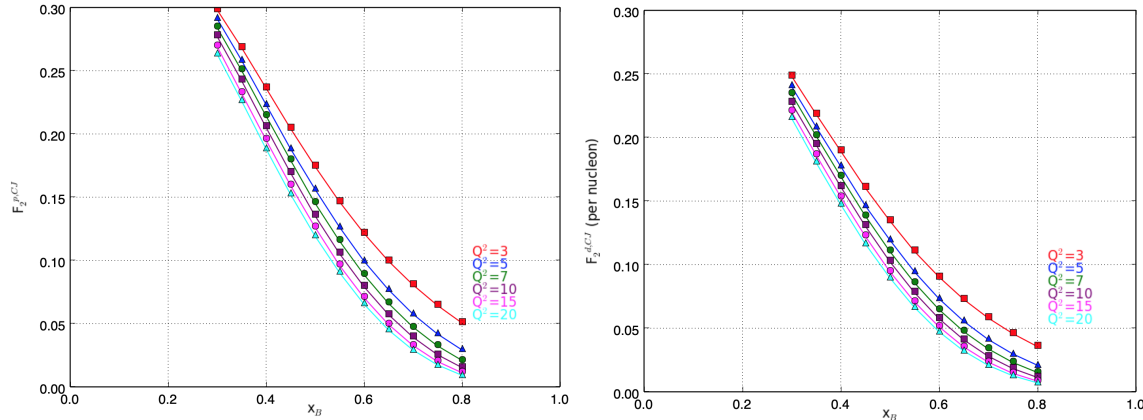


Figure 5: Left: The proton structure function from the CJ15 fit is shown as a function of x_B for various fixed Q^2 . Right: The deuteron structure function from the CJ15 fit is shown as a function of x_B for various fixed Q^2 .

deuteron structure functions both show clear differences for the same values of x_B over this range of Q^2 .

The nuclear effects of the proton and neutron in the deuteron can be directly characterized by dividing the deuteron structure function by the sum of the free proton and free neutron structure functions. The result is shown on the left in Fig. 6. Over the typical range of x_B that is relevant to the EMC Effect, the Q^2 dependence is minimal. At approximately $x_B = 0.6$ and greater, the ratio varies greatly with Q^2 .

The same ratio is shown on the right in Fig. 6 using the global Whitlow deuterium data. The same general trend is observed as that shown in the CJ15 where the Q^2 has a more significant effect on the ratio at large values of x_B . The F_2^d / F_2^p and F_2^d / F_2^n ratios from the CJ15 fit are shown in Fig. 7.

The significance of the spread in ratios at large x_B values is that many experiments, SLAC E139 included, did not observe a large Q^2 dependence in the data and so the points were averaged in Q^2 for each point in x_B . Additionally, the EMC Effect is characterized by a linear fit in the range

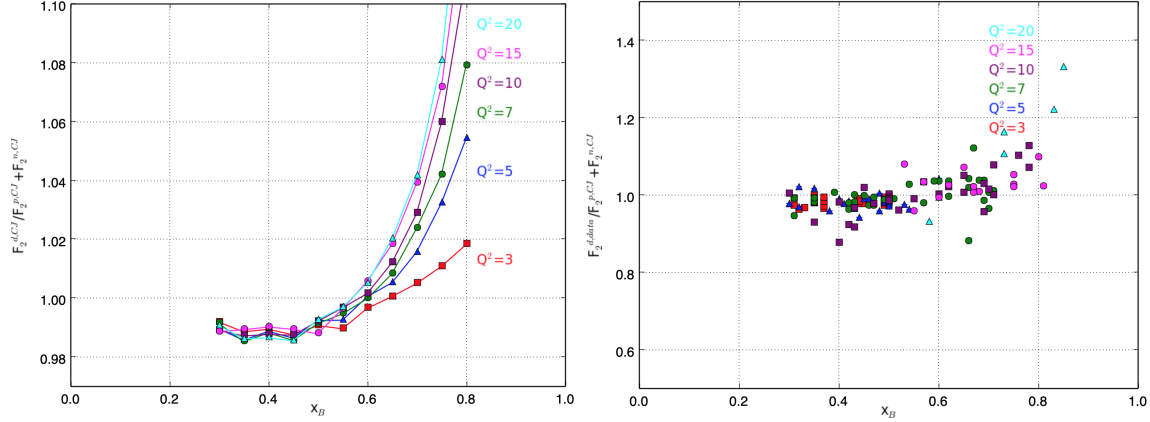


Figure 6: Left: The deuteron structure function divided by the sum of the free proton and free neutron structure functions from the CJ15 fit is shown for various Q^2 . This ratio roughly shows the magnitude of the nuclear effects in the deuteron. The Q^2 dependence shows significant spread above $x_B = 0.6$ where the ratio begins to increase. Right: The global Whitlow deuterium data from SLAC [7] is shown divided by the sum of the free proton and free neutron structure functions from the CJ15 fit.

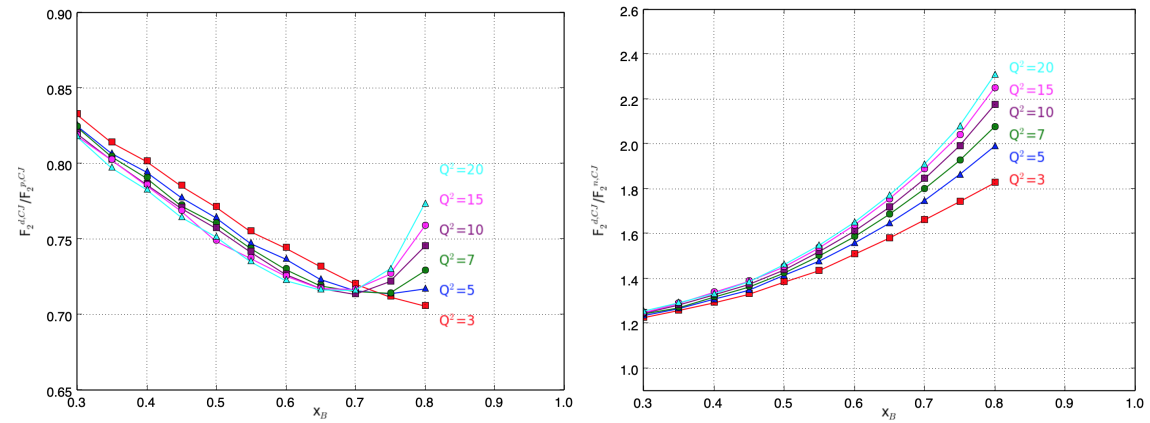


Figure 7: Left: The deuterium structure function from the CJ15 fit is shown as a ratio to the proton structure function from CJ15 for various Q^2 . Right: The deuterium structure function from the CJ15 fit is shown as a ratio to the neutron structure function from CJ15 for various Q^2 .

of x_B from 0.3–0.7 where deuterium clearly exhibits non-linear nuclear modification effects. These two observations affect the interpretation and extraction of the EMC Effect.

4 Structure function extraction from the E139 cross sections

Most experiments only publish the extracted F_2 ratios. For this analysis, the experimental cross sections were desirable for the flexibility to construct and study the F_2 ratios for the nucleus of interest relative to free nucleon quantities. The SLAC E139 experiment published the experimental cross sections for the following nuclei: deuterium, helium, beryllium, carbon, aluminum, calcium, iron, silver and gold. The cross sections include published statistical and systematic errors. The F_2 structure function for each nucleus is extracted from the cross section using the relationship shown in Equation (1).

$$F_2 = \frac{d^2\sigma}{d\Omega dE'} \frac{1+R}{1+\epsilon R} \frac{K\nu}{4\pi^2\alpha\Gamma(1+\nu^2/Q^2)} \quad (1)$$

From Equation (1), ϵ , K , and Γ are defined by the usual quantities of the electron scattering kinematics in Equation (4). These quantities include the measured scattering angle θ , the momentum transfer Q^2 , the energy transfer ν , the scattered electron energy E' , the mass of the proton M , and the squared invariant mass W^2 . R is determined from the R1990 fit to world data.

$$\epsilon = (1 + 2 \frac{\nu^2 + Q^2}{Q^2} \tan^2 \frac{\theta}{2})^{-1} \quad (2)$$

$$K = \frac{W^2 - M^2}{2M} \quad (3)$$

$$\Gamma = \frac{\alpha KE'}{2\pi^2 Q^2 E (1 - \epsilon)} \quad (4)$$

For most published cross section ratios, corrections are applied to account for the excess of neutrons in asymmetric nuclei. This correction is referred to as the “isoscalar correction” and is defined in Equation (5). While this correction is not applied in this paper for the F_2 ratios per free proton and free neutron, it is relevant for accurately reconstructing the published F_2^A/F_2^d cross sections as in most analyses. For all analysis in this paper, an additional requirement for $W^2 > 4$ GeV² was applied in order to ensure that the results obtained are above the resonance region.

$$f_{iso}^A = \frac{\frac{1}{2}(1 + F_2^n/F_2^p)}{\frac{1}{A}(Z + (A - Z)F_2^n/F_2^p)} \quad (5)$$

From the analysis described in this section, the carbon and gold F_2^A/F_2^d ratios are reconstructed (with the iso-scalar correction applied to gold) and compared to the published ratios in the EMC and NMC experiments as shown in Fig. 8.

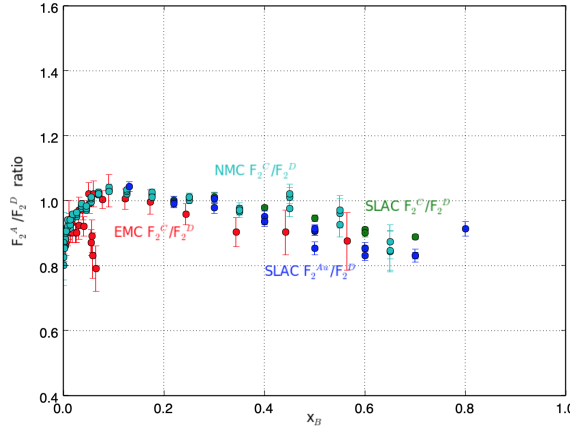


Figure 8: The published structure function ratios per nucleon for carbon and gold are shown from SLAC, NMC, and the EMC experiments.

The carbon ratio from the SLAC E139 experiment is consistent with the ratio found in the EMC and NMC experiments, and the carbon exhibits a shallower slope with respect to x_B as compared to the heavier, iso-scalar corrected gold ratio.

5 General observations

The standard EMC structure function ratio is compared with ratios of the structure function of the nucleus to that of the free proton and free neutron, separately. The F_2^A/F_2^d ratios for the carbon and gold nuclei are shown in Fig. 9 using the collective world data as published in Ref. ???. The gold nucleus (heavier than carbon) exhibits a steeper slope as a standard observation of the EMC Effect. The F_2^A/AF_2^p ratio is the per nucleon ratio to the proton structure function and is also shown in Fig. 9. These ratios are consistent with theory predictions and exhibit a similar trend to the ratio of the structure function to deuterium in that the slope steepens for heavier nuclei. The vertical spread in the ratios of the various nuclei lessens when an iso-scalar correction is applied. The F_2^p structure function is obtained from the CJ15 fit.

The F_2^A/AF_2^n ratio is the per nucleon to the free neutron. The free neutron F_2^n is from the CJ15 fit to the world data. As shown in Fig. 9, the F_2^A/AF_2^n ratios for the SLAC E139 nuclei exhibit a significantly larger vertical spread when compared to the vertical spread of the F_2^A/AF_2^p ratios for various nuclei. The F_2^A/AF_2^n ratios also exhibit a positive slope in contrast to the ratios constructed using the free proton. These observations are further magnified on the right in Fig. 9 where the ratios for each nuclei are shown as per proton (F_2^A/ZF_2^p) and per neutron (F_2^A/NF_2^n).

6 Deuterium nuclear effects and heavier nuclei

6.1. Deuterium

The nuclear effects in deuterium are non-negligible for values of x_B from 0.3–0.7 in the region of interest to the EMC Effect. The nuclear effects in deuterium can be quantified somewhat as the difference between the sum of the free proton and free neutron to that of the measured deuterium structure function. In Fig. 10, the F_2^A ratio is defined in two ways: the standard F_2^A/F_2^d (shown in

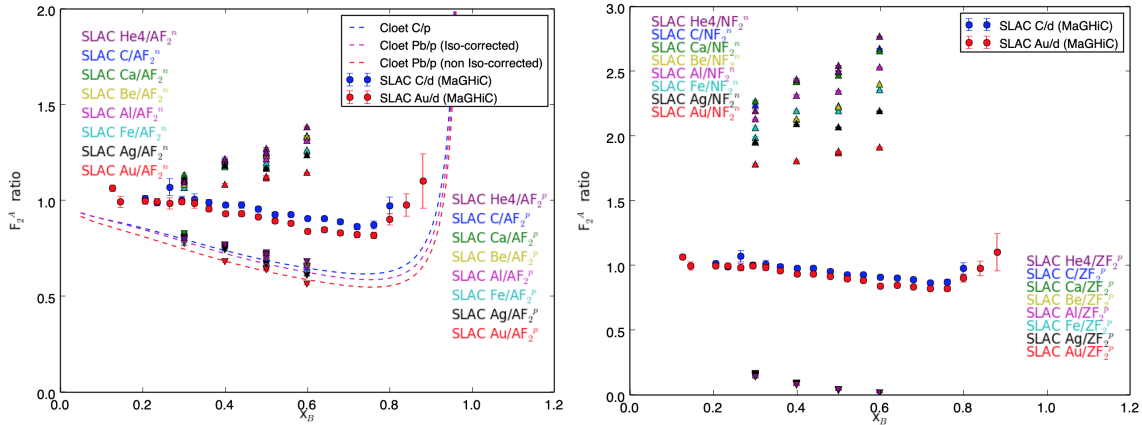


Figure 9: Left: F_2^A calculated from the published SLAC E139 cross sections is taken as a ratio per nucleon to F_2^n and F_2^p , separately. The published EMC ratios for carbon and gold [9] are shown for reference as F_2^A / F_2^d per nucleon. Theory predictions for the F_2^A structure function per nucleon as a ratio to F_2^p are shown. Right: F_2^A calculated from the published SLAC E139 cross sections is taken as a ratio per neutron or proton and F_2^n and F_2^p , separately. The published EMC ratios for carbon and gold [9] are shown for reference.

blue) and $F_2^A / ZF_2^p + (A - Z)F_2^n$ (shown in red). The SLAC E139 data was taken for Q^2 of 5, 10, and 15 GeV^2 .

In Fig. 10, the deuterium ratios from the SLAC E139 data are shown using the CJ15 structure function constructs in the denominators. The different Q^2 data are shown using different shapes in each plot, and fits to the ratios are taken separately including and excluding the highest x_B point at 0.7. There is a systematic offset from unity for deuterium taken as a ratio to itself, but the ratio is relatively flat across x_B . There exists a clear difference between the ratio taken relative to the deuteron structure function (blue) and the ratio taken relative to sum of the free neutron and free proton structure functions (red). The difference also exhibits a small spread in Q^2 .

6.2. Heavier nuclei

The ratios for all the target nuclei in the SLAC E139 experiment are compared where the denominator is deuterium and the denominator is the sum of the free proton and neutron contributions. Carbon is a symmetric nucleus, and the results are shown in Fig. 11.

No data was taken in the E139 experiment for carbon at $x_B > 0.6$. The slope is steeper for the ratio taken with respect to the sum of the free neutron and free proton components. A more extreme case is seen in the gold nucleus in Fig. 12.

For the gold nucleus, the slope of the fit the ratio taken with respect to the free neutron and free proton is shallower than the slope taken with respect to deuterium (as consistent with the general trend observed in carbon). When data is fitted for a range of Q^2 values, a noticeable striping at each point in x_B is apparent. Furthermore, the higher x_B data (also higher Q^2), no longer sit linearly with respect to the lower x_B data. In all nuclei (see Appendix), this discrepancy is most apparent for values of x_B at 0.7. This observation is similar to where one would expect to see the contributions from the deuteron nuclear effects as shown in Fig. 2. Similar fits are made to all the nuclei (shown in the Appendix). The resultant slopes are shown in Tables 1, 2, and 3. The slopes are shown as a function of A for the nuclei in Fig. 13.

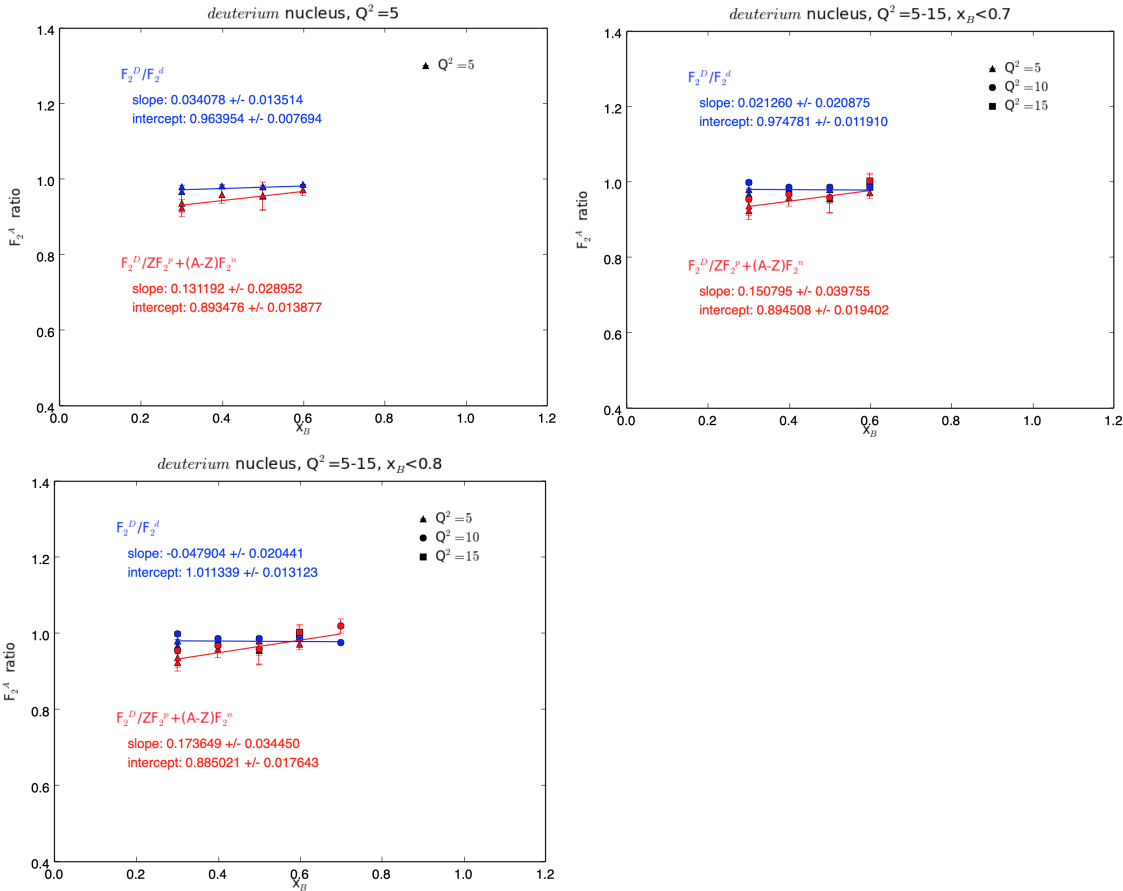


Figure 10: Linear fits to the deuterium target data with cuts on Q^2 and x_B . The blue data shows the ratio of the E139 nucleus relative to the CJ15 deuterium while the red data shows the ratio of the E139 nucleus relative to the sum of the free proton and free neutron (excluding nuclear effects of deuterium). Top left: linear fit to the data taken for $Q^2 = 5$ GeV^2 . Top Right: linear fit to the data taken for all Q^2 but excluding the data at $x_B = 0.7$. Bottom: linear fit to all data taken through $x_B = 0.7$.

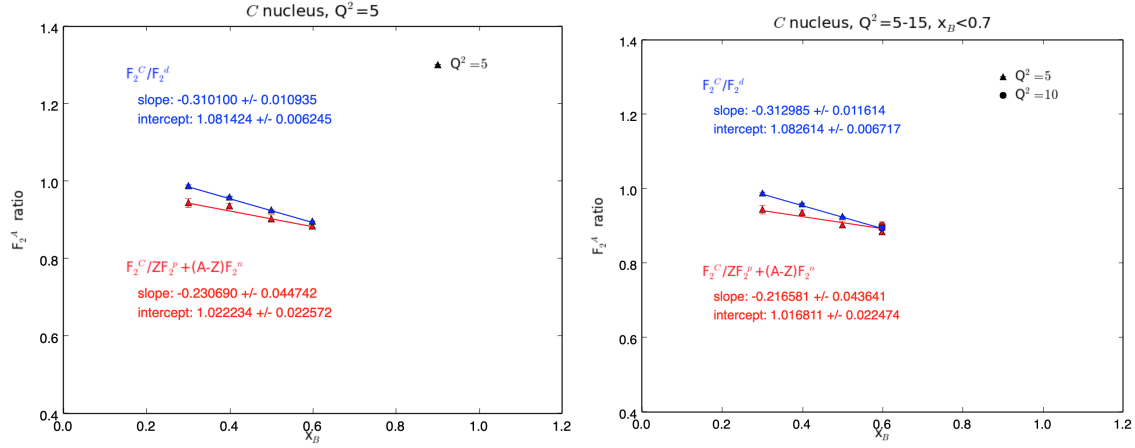


Figure 11: Linear fits to the C target data with cuts on Q^2 and x_B . The blue data shows the ratio of the nucleus relative to deuterium while the red data shows the ratio of the nucleus relative to the sum of the free proton and free neutron (excluding nuclear effects of deuterium). Left: linear fit to the data taken for $Q^2 = 5 \text{ GeV}^2$. Right: linear fit to the data taken for all Q^2 but excluding the data at $x_B = 0.7$. No data was taken in the E139 experiment for carbon at $x_B = 0.7$.

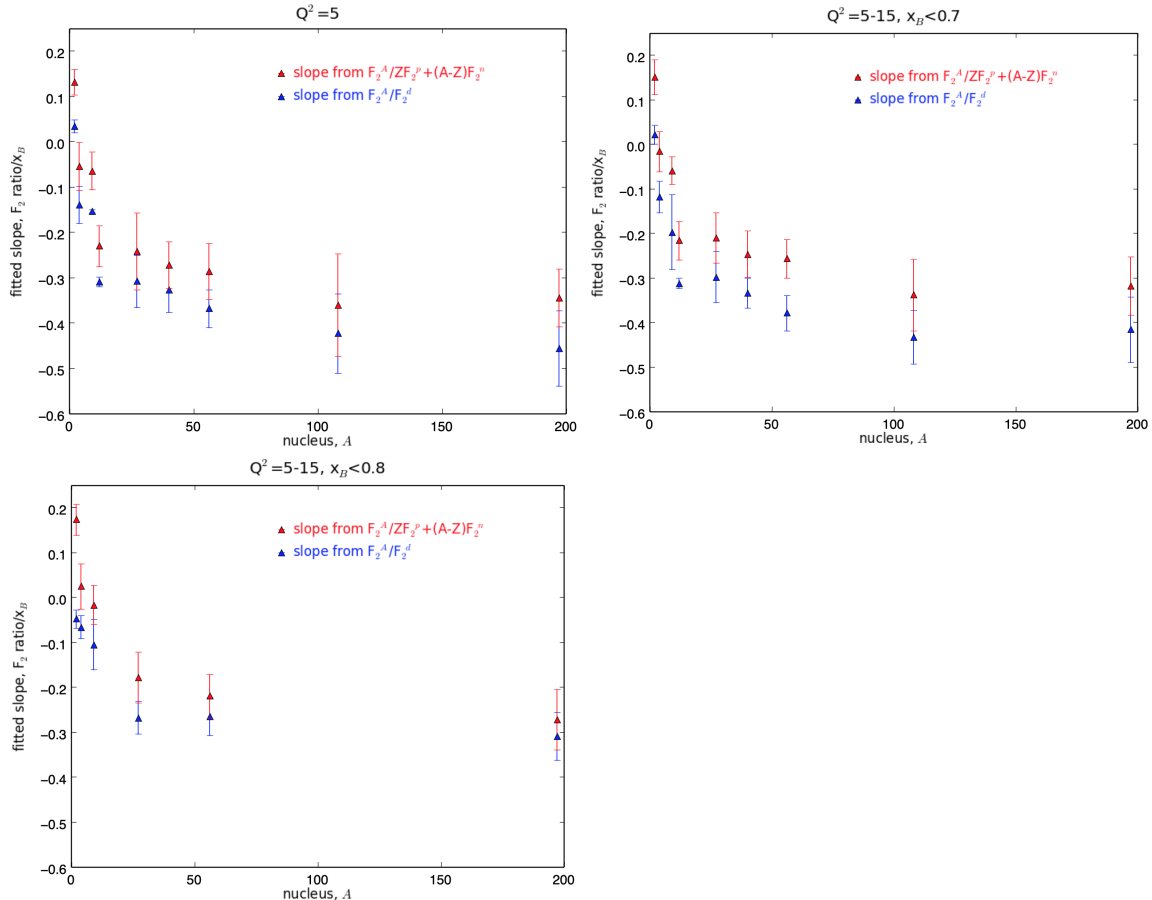


Figure 13: The slopes to the fits of the F_2 ratios versus x_B are shown for both denominators and as a function of the nucleus A . In all cases, the ratio taken with respect to the sum of the free neutron and free proton components exhibits a shallower slope than that taken deuterium.

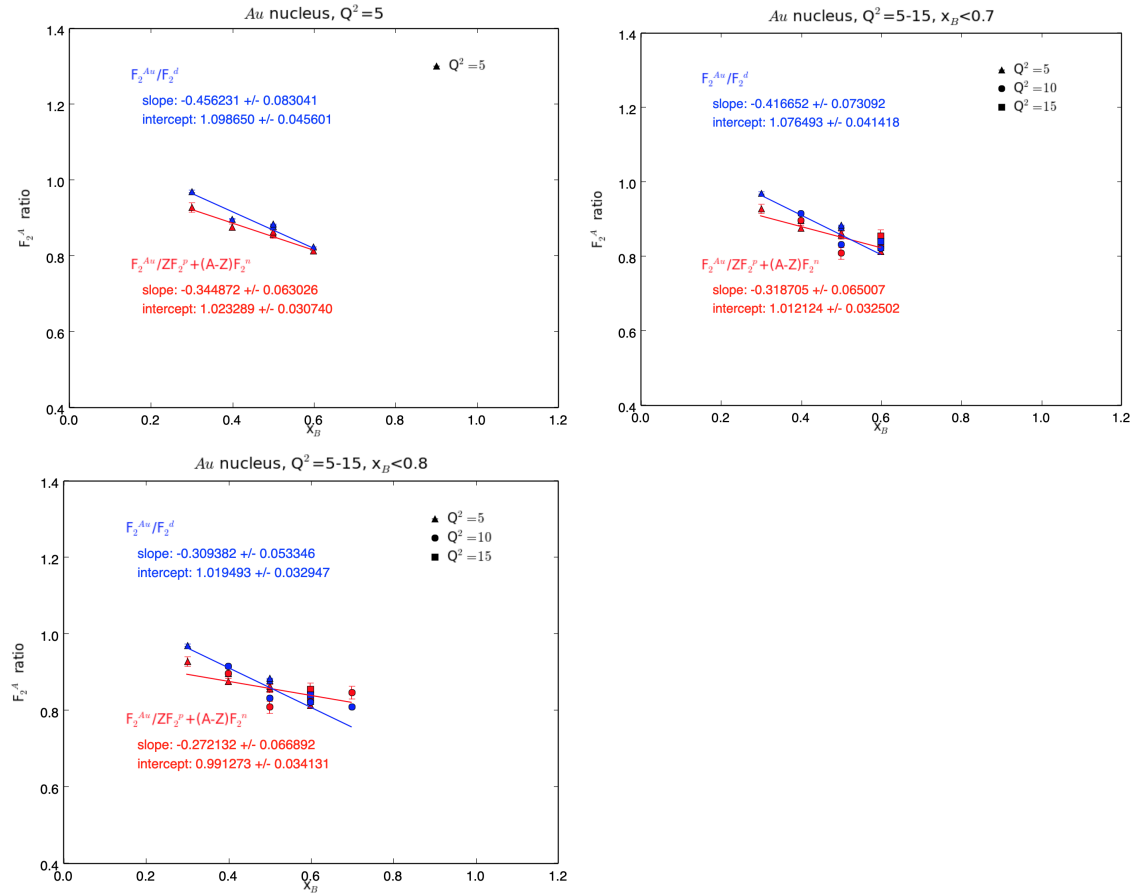


Figure 12: Linear fits to the Au target data with cuts on Q^2 and x_B . The blue data shows the ratio of the nucleus relative to deuterium while the red data shows the ratio of the nucleus relative to the sum of the free proton and free neutron (excluding nuclear effects of deuterium). Top left: linear fit to the data taken for $Q^2 = 5$ GeV^2 . Top Right: linear fit to the data taken for all Q^2 but excluding the data at $x_B = 0.7$. Bottom: linear fit to all data taken through $x_B = 0.7$.

The slopes for each ratio for various cuts in Q^2 and x_B are compared in Fig. 14. The inclusion of higher Q^2 and x_B data in the fits generates slightly shallower slopes due to the rise seen from the nuclear effects.

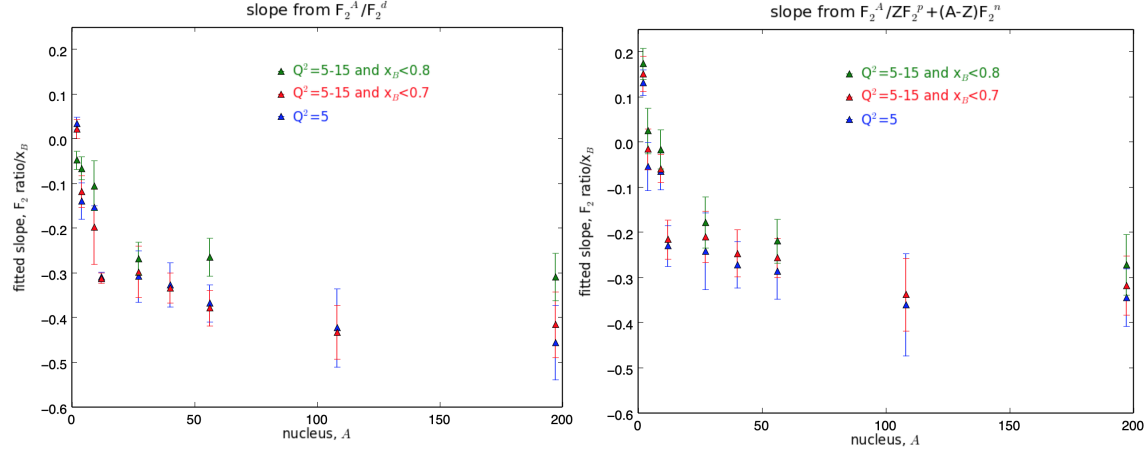


Figure 14: The slopes are compared for the different cuts in Q^2 and x_B . The inclusion of larger Q^2 and x_B points in the fit generates a somewhat shallower slope.

Table 1 shows the fitted slope and intercept values for both the F_2^A ratio for each nucleus taken with respect to deuterium and the sum of the free neutron and free proton contributions. In Table 1, only fits to the data where $Q^2 = 5$ are shown. No iso-scalar corrections are applied to the asymmetric nuclei.

Table 1: Summary of linear fits to x_B where $Q^2 = 5$.

Nucleus	A/d slope	A/d intercept	A/(n+p) slope	A/(n+p) intercept
deuterium	0.034078+/-0.013514	0.963954+/-0.007694	0.131192+/-0.028952	0.893476+/-0.013877
He4	-0.139559+/-0.041514	1.010444+/-0.023729	-0.054561+/-0.053741	0.947196+/-0.027083
Be	-0.153575+/-0.004225	1.020754+/-0.002375	-0.064459+/-0.041653	0.955925+/-0.020121
C	-0.310100+/-0.010935	1.081424+/-0.006245	-0.230690+/-0.044742	1.022234+/-0.022572
Al	-0.308688+/-0.058075	1.074479+/-0.032618	-0.241920+/-0.085474	1.021834+/-0.042052
Ca	-0.327402+/-0.048885	1.085172+/-0.027035	-0.27227+/-0.051774	1.037505+/-0.025103
Fe	-0.368335+/-0.041561	1.085849+/-0.022646	-0.286425+/-0.062250	1.024809+/-0.029771
Ag	-0.423013+/-0.087616	1.119710+/-0.048607	-0.360732+/-0.113255	1.068858+/-0.055132
Au	-0.456231+/-0.083041	1.098650+/-0.045601	-0.344872+/-0.063026	1.023289+/-0.030740

Table 2 shows the fitted slope and intercept values for both the F_2^A ratios where all E139 Q^2 data are included at $x_B < 0.7$.

Table 2: Summary of linear fits to x_B where $Q^2 = 5 - 15$ and $x_B < 0.7$.

Nucleus	A/d slope	A/d intercept	A/(n+p) slope	A/(n+p) intercept
deuterium	0.021260+/- 0.020875	0.974781+/- 0.011910	0.150795+/- 0.039755	0.894508+/- 0.019402
He4	-0.118090+/- 0.035769	0.997067+/- 0.020596	-0.016222+/- 0.045129	0.931353+/- 0.023103
Be	-0.197454+/- 0.083778	1.035493+/- 0.048067	-0.059106+/- 0.030303	0.953386+/- 0.015144
C	-0.312985+/- 0.011614	1.082614+/- 0.006717	-0.216581+/- 0.043641	1.016811+/- 0.022474
Al	-0.298244+/- 0.057500	1.070859+/- 0.032829	-0.210889+/- 0.056564	1.010775+/- 0.028368
Ca	-0.334267+/- 0.034303	1.088128+/- 0.019560	-0.247045+/- 0.051788	1.027656+/- 0.025990
Fe	-0.379082+/- 0.040058	1.085956+/- 0.022621	-0.257315+/- 0.043599	1.010276+/- 0.021402
Ag	-0.432939+/- 0.060259	1.124006+/- 0.034442	-0.338549+/- 0.081071	1.060178+/- 0.040839
Au	-0.416652+/- 0.073092	1.076493+/- 0.041418	-0.318705+/- 0.065007	1.012124+/- 0.032502

Table 3 shows the fitted slope and intercept values for both the F_2^A ratios where all E139 Q^2 data are included with no cuts on x_B .

Table 3: Summary of linear fits to x_B where $Q^2 = 5 - 15$ and $x_B < 0.8$.

Nucleus	A/d slope	A/d intercept	A/(n+p) slope	A/(n+p) intercept
deuterium	-0.047904+/- 0.020441	1.011339+/- 0.013123	0.173649+/- 0.034450	0.885021+/- 0.017643
He4	-0.066610+/- 0.025529	0.969128+/- 0.015975	0.024671+/- 0.050676	0.913125+/- 0.026599
Be	-0.105347+/- 0.056027	0.986067+/- 0.035211	-0.016830+/- 0.042937	0.934997+/- 0.022080
C	—	—	—	—
Al	-0.268256+/- 0.036285	1.054884+/- 0.022384	-0.178675+/- 0.057032	0.996550+/- 0.029163
Ca	—	—	—	—
Fe	-0.265522+/- 0.041894	1.026296+/- 0.025600	-0.219929+/- 0.048613	0.994104+/- 0.024310
Ag	—	—	—	—
Au	-0.309382+/- 0.053346	1.019493+/- 0.032947	-0.272132+/- 0.066892	0.991273+/- 0.034131

The slopes from Table 1 where $Q^2 = 5$ only are shown plotted against the SRC factor, a_2 . The general fitted slope is still linear across the a_2 values for each nucleus, but there is a clear systematic offset between the intercept values of these two fits. The fits to the slopes with respect to the SRC factor are shown in Fig. 15.

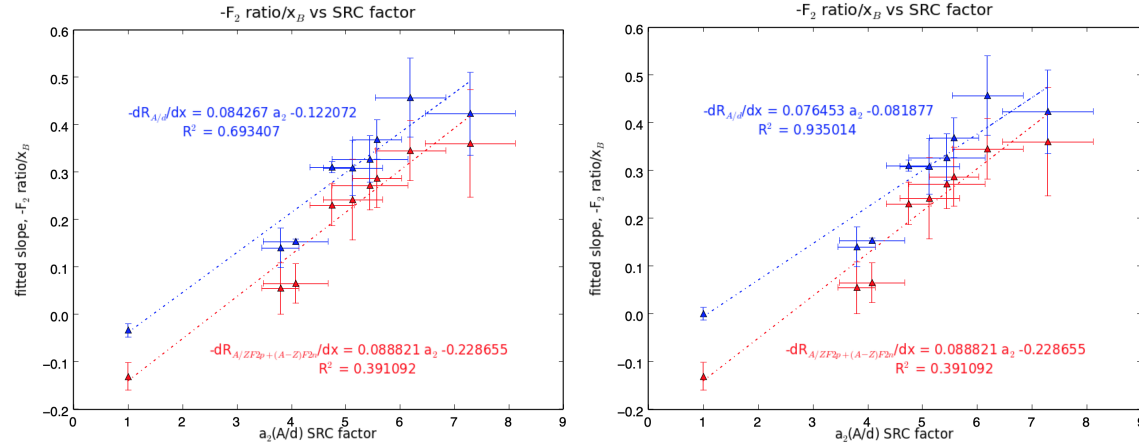


Figure 15: The slopes fit to the data for $Q^2 = 5$ are shown versus the a_2 SRC factor. Left: The slope value for deuterium is that which was obtained from the fits and corresponds to Table 1. Right: The slope value for deuterium is set to 0.

The intercept value of approximately -0.08 for the ratio taken with respect to deuterium when the deuterium point is set to 0 (Fig. 15 right) is consistent with previous studies. The intercept value is significantly smaller for the data where the original slope ratio was taken with respect to the sum of the free proton and free neutron contributions.

7 Conclusions

The CJ Collaboration has recently extracted the free neutron structure function from the world DIS data opening new windows for exploring the EMC Effect and deuteron nuclear effects. General observations show that the deuteron ratio to the sum of the free proton and free neutron structure functions has some dependencies with Q^2 . These dependencies have been generally ignored by previous experiments. The changes with Q^2 are most significant at large Q^2 and large x_B . As the EMC Effect is calculated from the slope of the nucleus to deuteron structure function ratio, there is an apparent contamination of these results due to the nuclear effects of the deuteron alone. Additionally, these effects imply that the structure function ratios at $x_B > 0.6$ do not follow the linear trend of the data where $x_B < 0.3$ and $x_B < 0.6$. Therefore, it would seem that the EMC Effect as calculated using the slope of the F_2^A/F_2^d ratio has an x_B and Q^2 dependence. Also, there appears to be a more significant spread in A in the data where the structure function of the nucleus is taken with respect to the neutron vs the proton. This spread arises from the drop in the ratio F_2^n/F_2^p as a function of x_B .

8 Acknowledgments

The authors would like to thank Shujie Li for constructing the most complete world F_2^n data set to date and Alberto Accardi and Wally Melnitchouk for providing crucial insights and interpretations for this analysis.

References

- [1] A. Accardi, L. T. Brady, W. Melnitchouk, J. F. Owens and N. Sato, Phys.Rev. D93 (2016) 114017
- [2] J. Gomez *et al.*, “Measurement of the A-dependence of deep inelastic electron scattering,” Phys. Rev. D **49**, 4348 (1994). doi:10.1103/PhysRevD.49.4348
- [3] K. A. Griffioen *et al.*, “Measurement of the EMC Effect in the Deuteron,” Phys. Rev. C **92**, no. 1, 015211 (2015) doi:10.1103/PhysRevC.92.015211 [arXiv:1506.00871 [hep-ph]].
- [4] J. G. Rubin, J. Arrington, “A New Extraction of Neutron Structure Functions from Existing Inclusive DIS Data,” doi: 10.1063/1.3631528 [arXiv:1101.3506v2 [nucl-ex]].
- [5] L.W.Whitlow, SLAC-Report-357, Ph.D. Thesis, Stanford University, March 1990.
- [6] <https://www.slac.stanford.edu/exp/e139/E139.RESULTS>
- [7] http://www.slac.stanford.edu/exp/e140/SIGMA.D2_357
- [8] Alekhin, S. I. and Kulagin, S. A. and Petti, R., “Nuclear effects in the deuteron and constraints on the d/u ratio,” Phys. Rev. D **96**, no. 5, 0054005 (2017) doi:10.1103/PhysRevD.96.054005 [arXiv:1704.00204].
- [9] S. Malace, D. Gaskell, D. W. Higinbotham and I. Cloet, “The Challenge of the EMC Effect: existing data and future directions,” Int. J. Mod. Phys. E **23**, no. 08, 1430013 (2014) doi:10.1142/S0218301314300136 [arXiv:1405.1270 [nucl-ex]].

9 Appendix

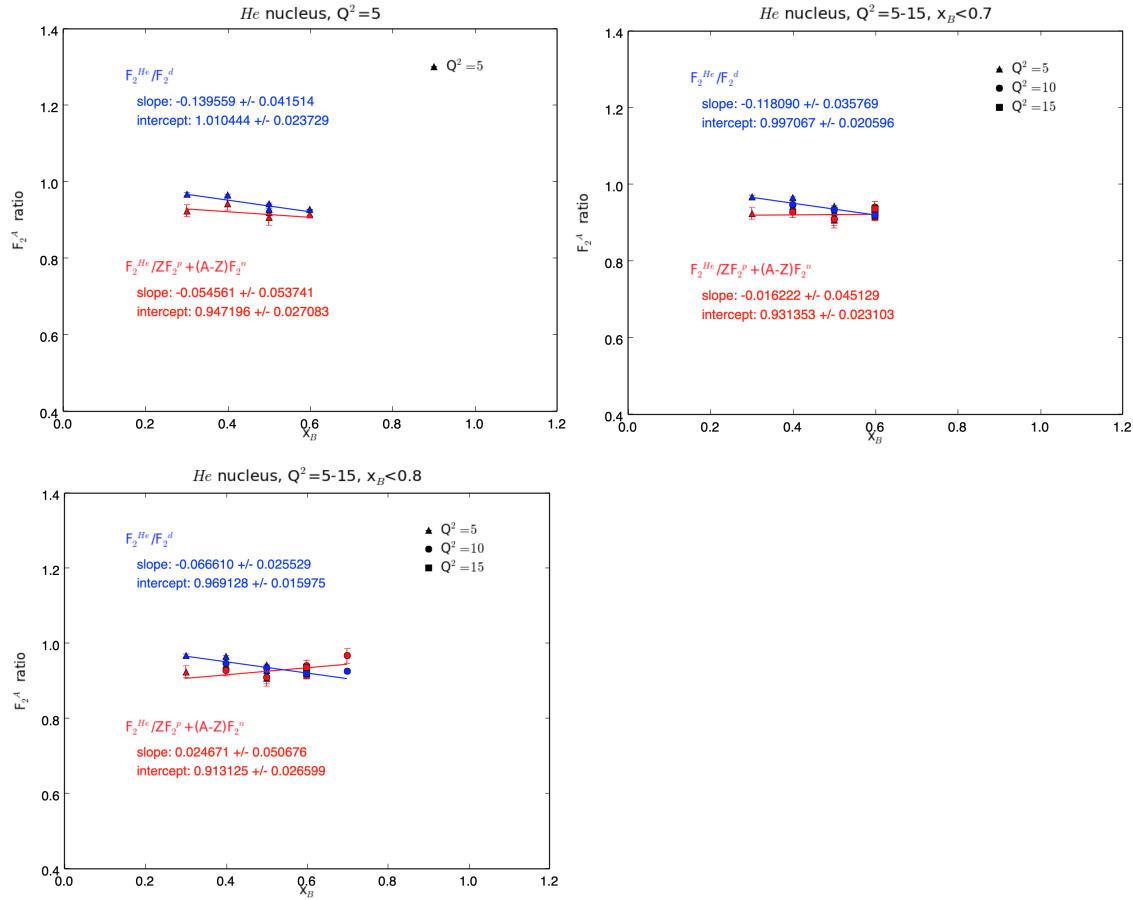


Figure 16: Linear fits to the He target data with cuts on Q^2 and x_B .

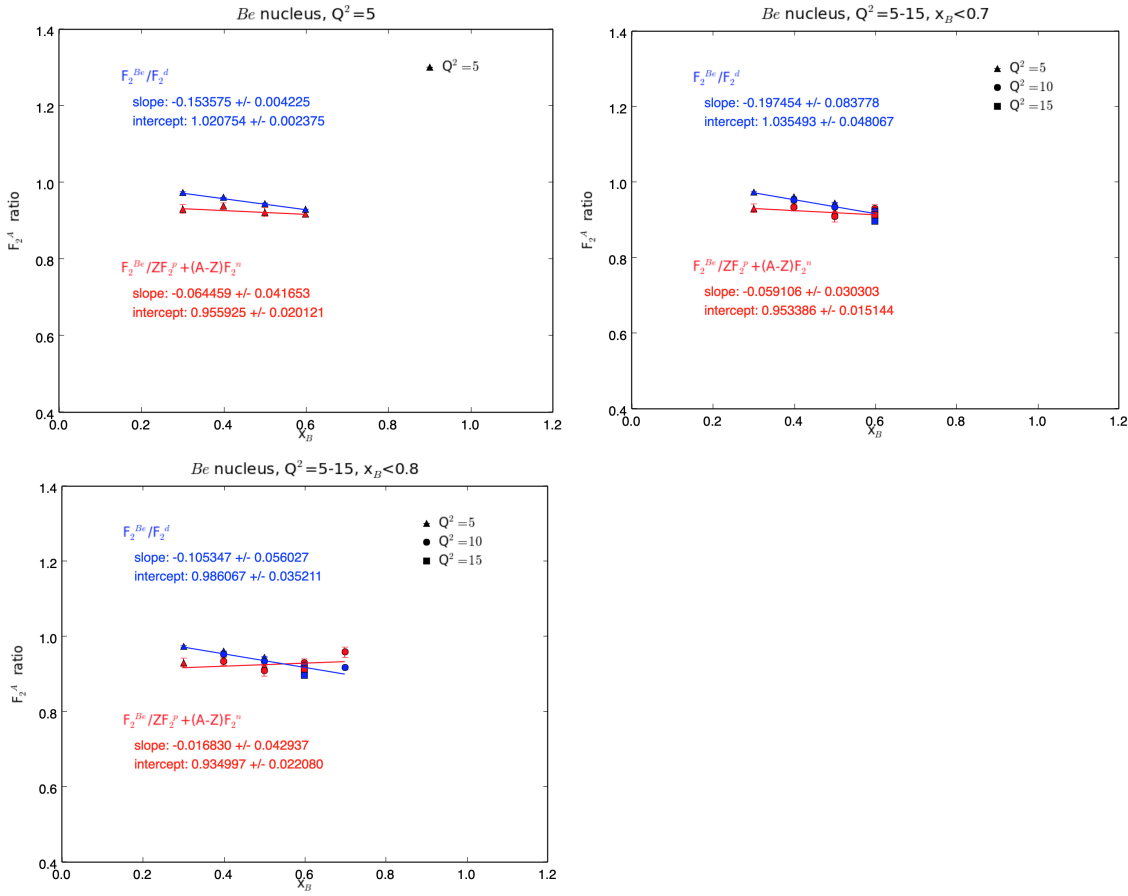


Figure 17: Linear fits to the Be target data with cuts on Q^2 and x_B .

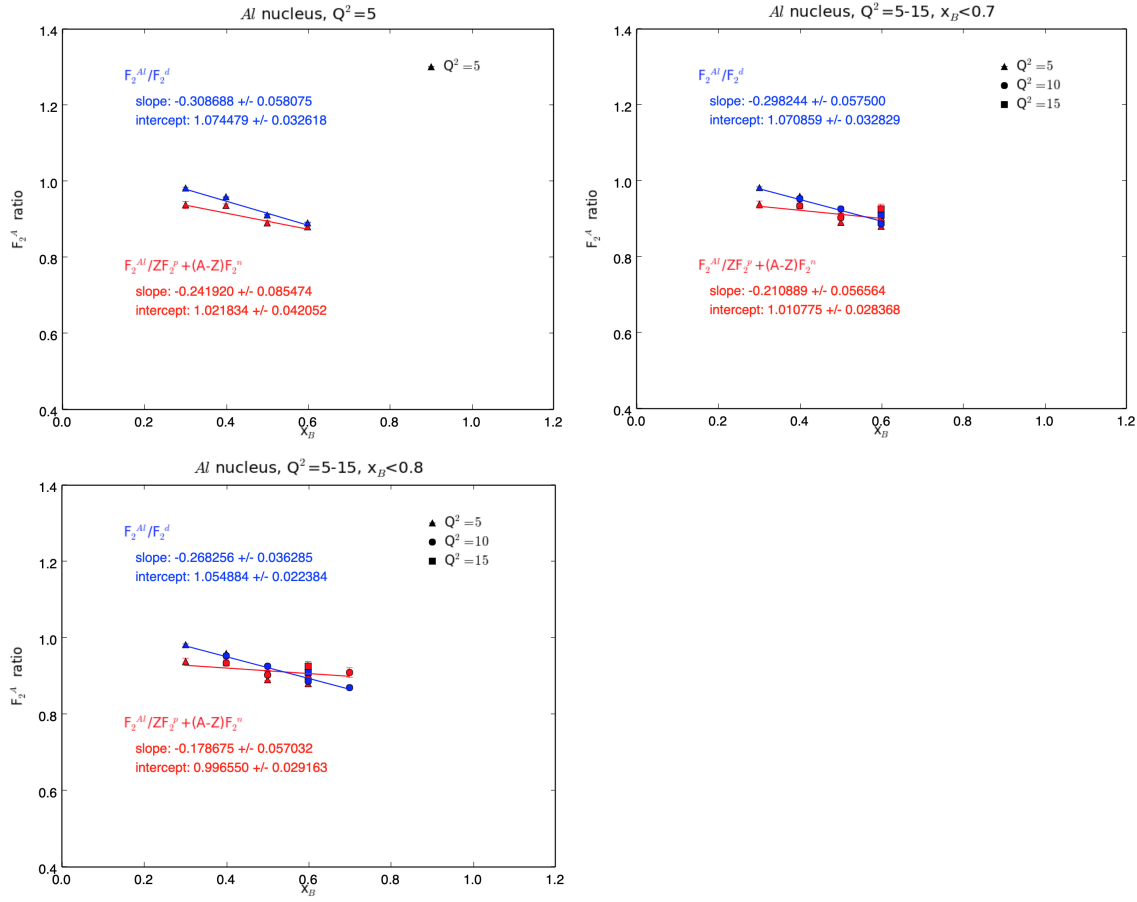


Figure 18: Linear fits to the Al target data with cuts on Q^2 and x_B .

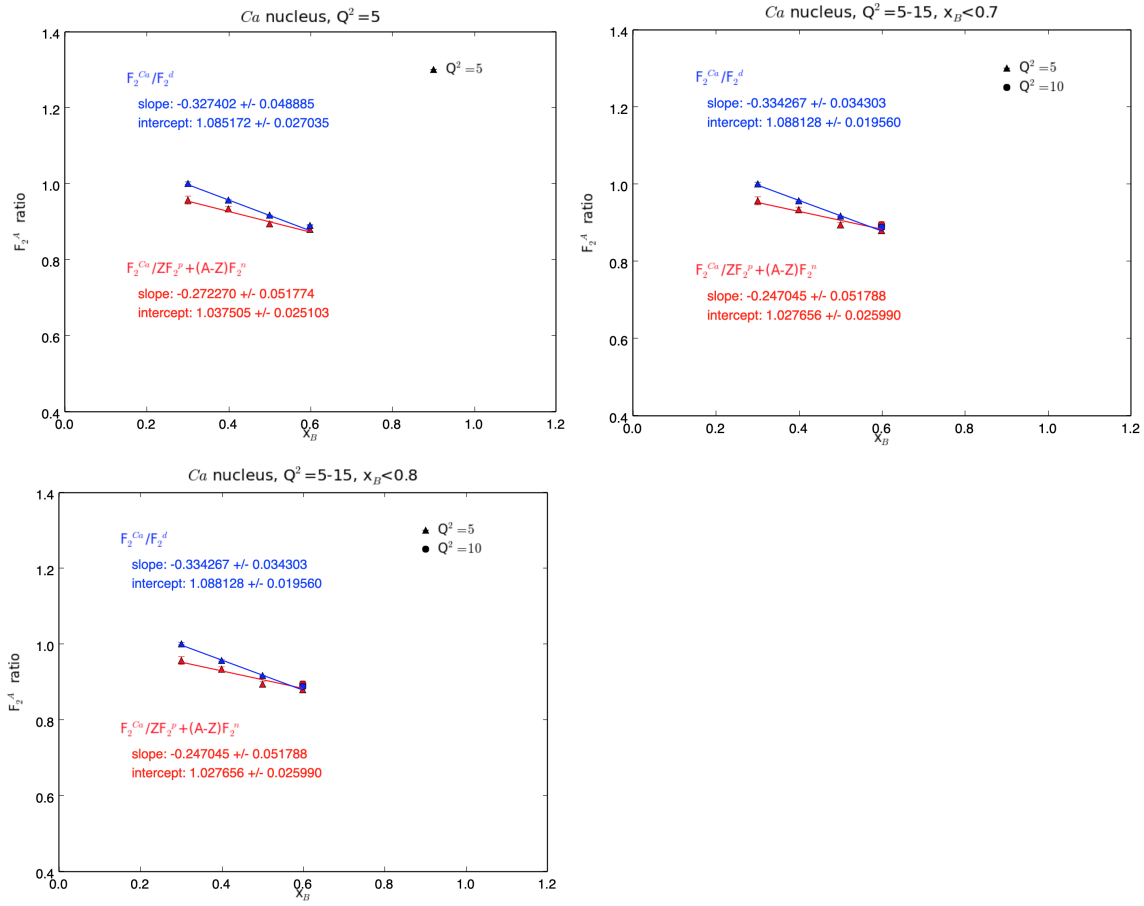


Figure 19: Linear fits to the Ca target data with cuts on Q^2 and x_B .

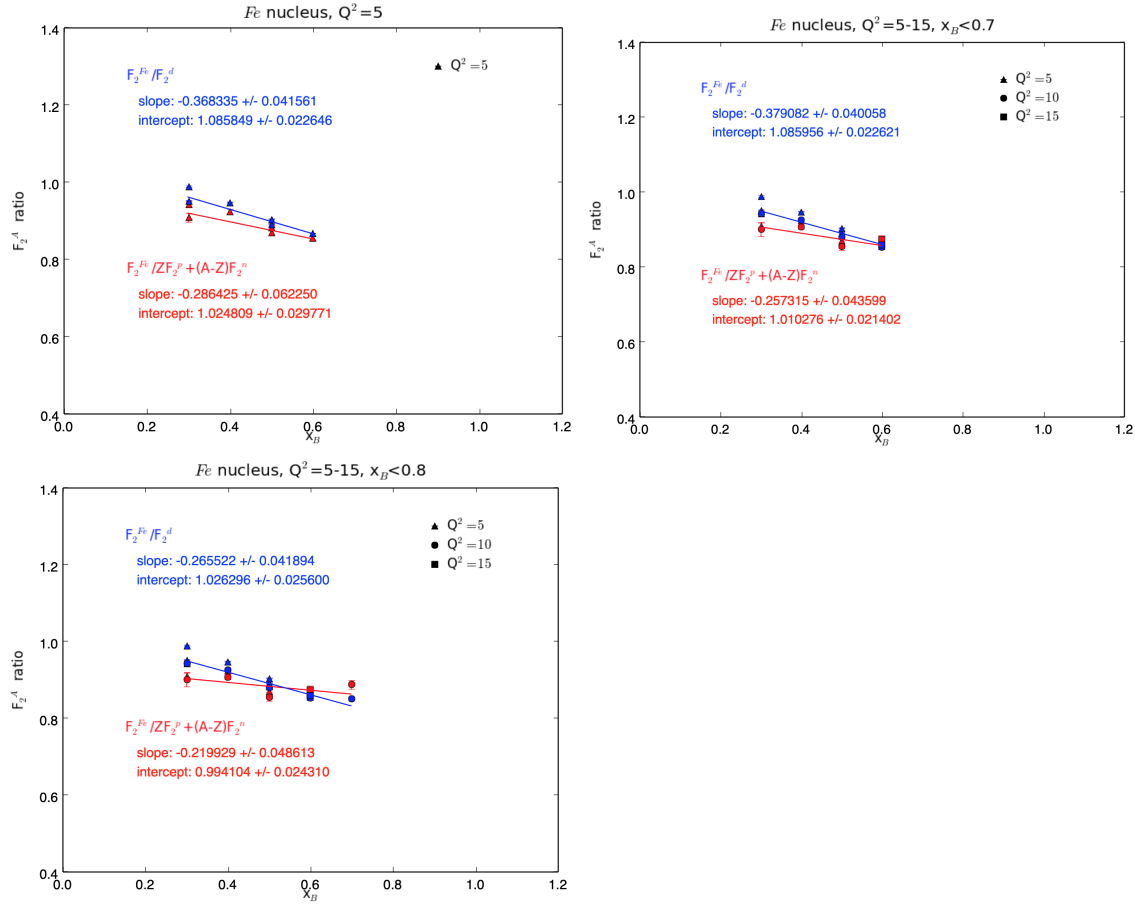


Figure 20: Linear fits to the Fe target data with cuts on Q^2 and x_B .

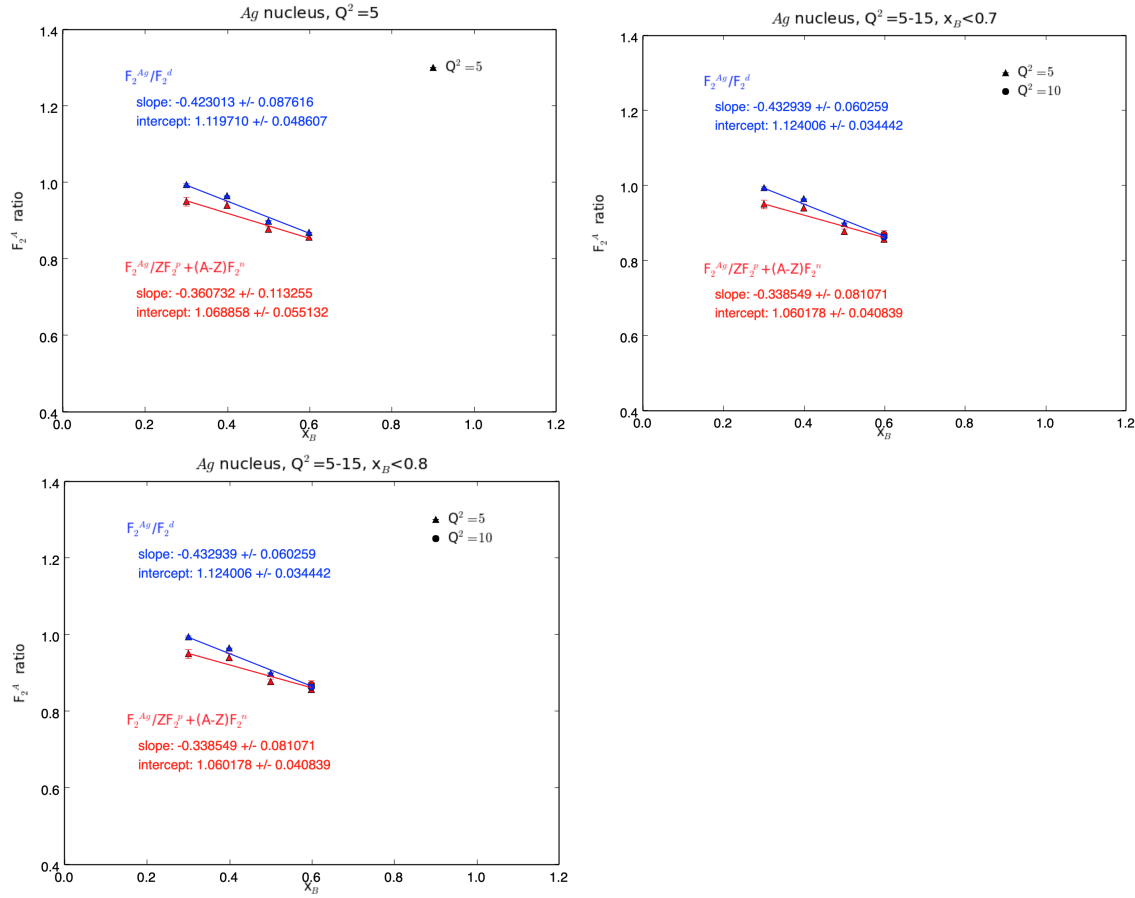


Figure 21: Linear fits to the Ag target data with cuts on Q^2 and x_B .